EPJ Web of Conferences **314**, 00033 (2024) https://doi.org/10.1051/epjconf/202431400033
QCD@Work 2024

Silica aerogel characterization for the ePIC dRICH detector

Anna Rita Altamura[1,*], on behalf of the ePIC dRICH Collaboration

[1]Istituto Nazionale di Fisica Nucleare, sezione di Bari, Italy

Abstract. The ePIC detector is specifically designed to address the entire physics program at the Electron-Ion Collider (EIC) and features several sub-detectors, including the dual-radiator Ring Imaging Cherenkov (dRICH) detector for high-momentum particle identification. Silica aerogel is chosen as the solid radiator due to its crucial optical properties. Ongoing research aims to optimize these characteristics, focusing on the transmittance measurements of aerogel tiles with varying refractive indices and the associated measurement setup.

1 Introduction

Ring Imaging Cherenkov (RICH) detectors identify charged particles by utilizing Cherenkov radiation, which occurs when charged particles move faster than the phase speed of light in a medium[1]. Traditional gas and liquid radiators have refractive indices either below 1.0018 (C_5F_{12}) or above 1.27 (liquid C_6F_{14})[1]. Silica aerogel emerges as the only practical solution to bridge this refractive index gap, avoiding the challenges of high-pressure gases or liquefied forms. Consisting of 99.8% air and 0.2% silicon dioxide, silica aerogel offers a compact structure with good optical transmittance and a low refractive index, making it the preferred choice for many RICH detectors.

2 Aerogel optical properties

The transmittance of silica aerogel quantifies how much light can pass through the material without absorption or scattering. Its unique structure features a three-dimensional lattice of interconnected nanopores, with diameters ranging from 2 to 50 nm[2]. This architecture allows visible light to travel with minimal scattering and absorption, enabling propagation with low attenuation. Light in silica aerogel mainly experiences Rayleigh scattering, where light is elastically scattered by particles much smaller than its wavelength.

Transmittance typically peaks in the near-infrared spectrum, where the silica network shows minimal radiation absorption. The relationship between aerogel transmittance T and the wavelength λ of the impinging radiation traversing a sample with thickness t is usually described using the Hunt formula[3]:

$$T(\lambda) = e^{-\frac{t}{\Lambda_T}} = Ae^{-\frac{C \times t}{\lambda^4}} \quad (1)$$

*e-mail: anna.rita.altamura@cern.ch

Table 1. List of the tiles under tests with their refractive index and nominal thickness *t*.

Tile	*n*	t [cm]	Tile	*n*	t [cm]
1	1.03	20.7	23	1.02(*2021*)	2.05
2		2.08	24		2.08
3		2.01	25		2.08
4		2.05	26		2.08
5		2.04	27	1.02(*2022*)	2.05
6		0.98	28		2.06
7		0.97	29		2.04
8	1.04	2.03	30		1.95
9		2.05	31		1.99
10		2.03	32		2.17
11		2.04	33		2.14
12		2.05	34		2.14
13	1.05	2.05	35		2.13
14		2.07	36		2.12
15		2.06	37		1.91
16		2.06	38		1.94
17		2.08	39		2.03
18	1.005	2.00	40		2.03
19		2.06	41		2.04
20		2.06	42		1.97
21	1.03	2.02			
22		2.03			

Here, C accounts for aerogel clarity, A for light absorption, and Λ_T is the "transmission length," indicating the distance light can travel with minimal absorption or scattering. High optical quality samples have A close to 1 and C near 0. Silica aerogel exhibits low absorption due to the minimal impurities in its silica network.

Additionally, the tiles studied are hydrophobic, repelling water and thus maintaining transparency in humid conditions. This property prevents water infiltration, which can scatter light and reduce transmittance.

The scattering and absorption capabilities can be assessed through the transmission length Λ_T:

$$\frac{1}{\Lambda_T} = \frac{1}{\Lambda_{scat}} + \frac{1}{\Lambda_{abs}}, \tag{2}$$

where Λ_{scat} is the scattering length and Λ_{abs} is the absorption length of the sample.

The Hunt formula (Eq. 1) assumes a Rayleigh scattering cross-section dependence on λ^4 and an absorption cross-section independent of the radiation wavelength. Consequently, A remains unaltered with variations in the wavelength of photons.

3 Aerogel characterization

We have characterized several 10×10 cm^2 and 15×15 cm^2 aerogel tiles with various refractive indeces at CERN in July 2022. Table 1 reports a list of the tested samples, where for each tile its refractive index and expected thickness in the center point of the tile are reported. Tiles from 1 to 17 were produced by Aerogel Factory Co. Ltd (Chiba, Japan) and delivered in March 2021[4][5], except tiles 6 and 7 which belongs to a production manufactured by Matsushita Electric Works (Japan) in 2000.

For practical reasons, this section will primarily focus on the results obtained for tile 1 and tile 2, which are composed of aerogel with a refractive index of 1.03. Any difference between tiles 1 and 2 and the other tiles will be highlighted.

3.1 Transmittance

Transmittance measurements were performed using a Perkin Elmer Lambda 650 spectrophotometer with an integrating sphere. A deuterium light source covered the spectrum from 250

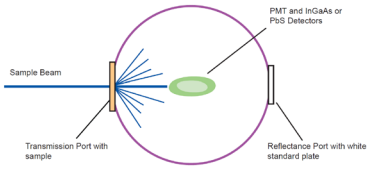

(a) Total transmittance.

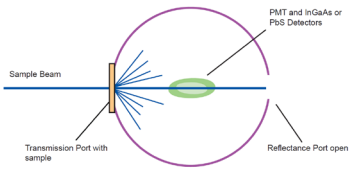

(b) Diffuse transmittance

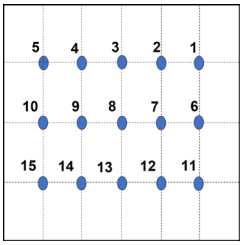

(c) Sampling points.

Figure 1. Schematic of total and diffuse measurement setup (left) and sampling points identification on the tile (right)

to 300 nm, while a halogen source was used for 300 to 800 nm, with measurements taken at 5 nm intervals. The aerogel sample was positioned in the transmission port at the sphere's entrance. As light passes through, it undergoes partial forward scattering, backward scattering, or absorption, with detection performed by a photomultiplier tube (PMT) at the sphere's bottom.

Total transmittance was measured with the reflectance port closed to prevent beam escape, as shown in Fig. 1a. The diffuse contribution was then measured by removing the reflectance port, allowing for the detection of only the diffuse light component, as depicted in Fig. 1b. Finally, the linear transmittance was calculated as the difference between total and diffuse transmittance.

Transmittance was measured at 15 different sampling points on each tile (identified in Fig. 1c) to assess its dependence on thickness and light wavelength (ranging from 250 to 800 nm). The overall transmittance for each tile at a given wavelength was calculated by averaging the values from the sampling points. This average was then fitted using the Hunt formula outlined in Eq. 1. However, small discrepancies were observed in the fit, as shown in Fig. 2. These discrepancies may stem from the assumption of a constant absorption term across the wavelength spectrum. To address this, a new term was introduced to account for absorption, considering the absorption length to vary with λ^8 as proposed in [3], leading to the *extended Hunt formula*:

$$T(\lambda) = e^{-\frac{t}{\Lambda_{\text{abs}}}} e^{-\frac{t}{\Lambda_{\text{scat}}}} = Ae^{-\frac{Bxt}{\lambda^8}} e^{-\frac{C\times t}{\lambda^4}} \tag{3}$$

A comparison between the fit using the standard Hunt formula and its extended version is presented in Fig. 2 for tile 1 with a refractive index of $n = 1.03$. It is evident that the extended Hunt formula provides a significantly better fit to the data compared to Eq. 1.

3.2 Thickness

In Fig. 3, a schematic illustrates the metrologic measurements taken at various points on tile 1, highlighting its concave shape. Indeed, both sides (A and B) of the tile have a curvature

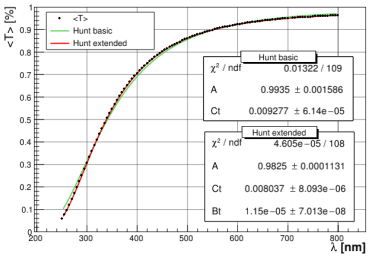

Figure 2. Transmission data of tile 1 (n = 1.03) fitted by both basic Hunt formula (green line) and its extended version (red line) including an additional absorption term.

Figure 3. Concave geometry of tile 1 obtained with metrology measurement (left) and vectors normal to the aerogel tile 1 on the exit side of the tile (right).

and this might have an impact on the resolution of the Cherenkov angle measurement in RICH applications, which can be slightly affected by the geometry and shape of the aerogel tile. The exit side's curvature, visible in Fig. 3, is crucial for estimating the normal vectors to the surface, which can enhance the accuracy of photon direction simulations.

The influence of the sample's shape on transparency is illustrated in Fig. 4, which shows tile 1 alongside the transmittance dispersion at the sampling points. The tile exhibits a thickness variation of approximately 0.5 mm, with greater thickness near the edges. As seen in Fig. 4, thicker areas correspond to lower transmittance, while thinner sections yield higher values. However, the overall variations in transmittance across the tile are minimal, with a spread of less than 1%, indicating a fairly uniform transmittance despite the tile's concave shape.

Considering a concave-shaped configuration, it is expected that point 8 (located at the center of the tile, as shown in Fig. 1c) would exhibit the smallest thickness. Consequently, when fitting the measured transmittance at point 8 using the Hunt extended formula, the thickness was constrained to its minimum value. Subsequently, the fit parameters (A, B, and C) obtained from this process were utilized to determine the thickness at all other sampling points across the entire tile.

3.3 Transmission length

Another way to address the impact of scattering and absorption on transmittance is through the transmission length Λ_T. This parameter is determined by both the absorption length Λ_{abs} and the scattering length Λ_{scat}, as illustrated in Eq. 2. In our model, we made the assumption that the scattering length varies with λ^4, and the absorption length is dependent on λ^8.

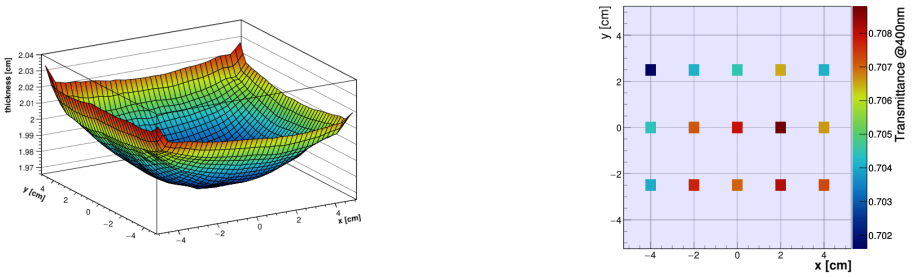

Figure 4. Comparison between tile thickness (left) and transparency dispersion (right). The measurements refer to tile 1 with n=1.03.

The lengths associated with transmission, scattering, and absorption were determined from the transmittance measurements. These parameters were obtained by fitting the transmittance curve as a function of wavelength, as described in Eq. 3:

$$\Lambda_T = -\frac{t}{ln(T(\lambda))}, \qquad \Lambda_{scat} = \frac{\lambda^4}{C}, \qquad \Lambda_{abs} = \frac{\lambda^8 t}{Bt - \lambda^8 lnA}$$

In this case, we used the average thickness value obtained from the metrology measurements to estimate the transmission, absorption, and scattering lengths.

3.4 Comparison

While we have focused on presenting the results for tiles 1 and 2, a comprehensive comparison of the results obtained from all the tested tiles can yield valuable insights into how the optical properties of the aerogel vary as a function of the refractive index.

In Fig. 5, we present the outcomes of the transmittance measurements for all the tested tiles, plotted as a function of the wavelength. These results show an overall increase in transmittance, even though distinctions can be found among tiles with different refractive indices.

The transmittance measurements reveal that tiles with a refractive index of $n = 1.03$ (tiles 1-5) generally exhibit higher transmittance values at 400 nm compared to all the other tiles. However, two notable exceptions are observed: tiles 6 and 7, featuring larger transmittance than the other tiles with $n = 1.03$ due to their thickness, and the tiles with a very low refractive index of $n = 1.005$, which exhibit significantly lower transmittance values due to the old manufacturing technology used.

A clear distinction among the tiles is further emphasized in Fig. 5, where the transmission length at 400 nm is plotted as a function of the refractive index. Tiles with a refractive index of $n = 1.03$ exhibit notably larger transmission lengths compared to the other tiles. As already mentioned, tiles with $n = 1.03$ and a thickness of 1 cm (tiles 6-7) show significantly shorter transmission lengths if compared to the ones with same refractive index and 2 cm.

We can also compare the transmission length values obtained through our evaluation with those provided by the manufacturers (nominal values). In particular, our extracted values tend to be slightly lower than the nominal values for nearly all the tiles. This variance could potentially arise from the thickness value employed in our calculations or from uncertainties related to the assumption that the transmittance value is an average taken from the 15 sampling points.

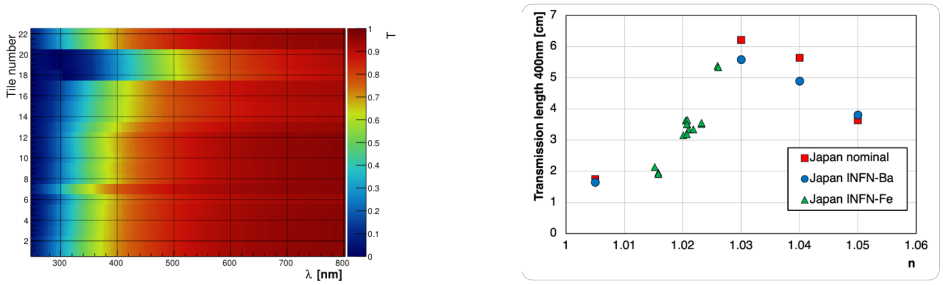

Figure 5. Transmittance as a function of the wavelength for all the tiles (left) and Λ_T at 400 nm as a function of the refractive index.

4 Conclusion

This study investigates the optical properties of several silica aerogel tiles with varying refractive indices. Initially, the transmittance curve was fitted as a function of wavelength, necessitating a new approach for improved accuracy. An additional term was incorporated into the basic Hunt formula to account for photon absorption, significantly enhancing the fit quality. The extended Hunt formula was then used to calculate the transmission, absorption, and scattering lengths for each tile, while the average thickness was determined from multiple measurements across each tile.

The results indicate that aerogel samples with refractive index n=1.03 demonstrates higher transmittance and longer transmission lengths. Indeed, at this refractive index, transmission lengths reach their maximum, while scattering and absorption probabilities are minimized. Notably, transmission lengths exceeded tile thickness significantly, demonstrating aerogel's potential as a radiator in Cherenkov detectors. Additionally, the absorption length was much greater than the scattering length, suggesting that absorption's impact is negligible.

Overall, advancements in high-quality hydrophobic silica aerogel make it an excellent candidate for Cherenkov applications, balancing a low momentum threshold for emission and a high photon yield for improved angular resolution in particle identification.

References

[1] E. Nappi and J. Seguinot. "Ring imaging Cherenkov detectors: The state of the art and perspectives". In: *Riv. Nuovo Cim.* 28.8-9 (2005), pp. 1–130. DOI: 10.1393/ncr/i2006-10004-6

[2] Jyoti Gurav et al. "Silica Aerogel: Synthesis and Applications". In: *Journal of Nanomaterials* 2010 (Aug. 2010). DOI: 10.1155/2010/409310

[3] E. Nappi. "Aerogel and its applications to RICH detectors". In: *Nucl. Phys. B Proc. Suppl.* 61 (1998). Ed. by E. Borchi et al., pp. 270–276. DOI: 10.1016/S0920-5632(97)00573-2

[4] Ichiro Adachi. "Status of high-quality silica aerogel radiators". In: *NIM-A* 952 (2020), p. 161919. ISSN: 0168-9002. DOI: https://doi.org/10.1016/j.nima.2019.02.046

[5] Makoto Tabata et al. "Development of transparent silica aerogel over a wide range of densities". In: *NIM-A* 623.1 (2010), pp. 339–341. ISSN: 0168-9002. DOI: https://doi.org/10.1016/j.nima.2010.02.241